Comparative study of the structural and physicochemical properties of two food derived antihypertensive tri-peptides, Isoleucine-Proline-Proline and Leucine-Lysine-Proline encapsulated into a chitosan based nanoparticle system

Minna Khalid [a b], Giuliana Vozza [a b], Hugh J. Byrne [b], Jesus M. Frias [a], Sinéad M. Ryan [c]

[a] School of Food Science and Environmental Health, Dublin Institute of Technology, Marlborough Street, Dublin 1, Ireland

[b] FOCAS Research Institute, Dublin Institute of Technology, Kevin Street, Dublin 8, Ireland

[c] School of Veterinary Medicine, University College Dublin, Belfield. Dublin 4, Ireland

[*] Corresponding author. E-mail: jesus.frias@dit.ie

Abstract

Food derived tri-peptides; Leucine-Lysine-Proline (LKP) and Isoleucine-Proline-Proline (IPP) are angiotensin converting enzyme inhibitors and may have potential to attenuate hypertension. The aim of this work was to understand the interactions of IPP and LKP when formulated into a CL113 nanoparticle (NP) to help improve permeation. Our findings indicate different IC_{50} values (LKP: 0.36 ±0.01 μM and IPP: 3.1 ±0.6 μM) and encapsulation efficiencies at different ratios of CL113: tripolyphosphate (LKP NPs: 65% at 6:1 and IPP NPs: 43% at 4:1). Molecular modelling and circular dichroism showed different stable amino side-chain-specific conformations for each peptide. IPP showed more steric hindrances to intra-chain rotations, resulting in an unordered peptide structure, whereas LKP showed more flexibility associated with a (disordered) β-strand-like conformer. *In-vitro* release kinetics showed a slower release for LKP NPs in acidic pH compared to IPP NPs. In conclusion, LKP NPs were found to have better binding compatibility with CL113.

Keywords: Leucine-Lysine-Proline (LKP); Isoleucine-Proline-Proline (IPP); bioactive peptides; chitosan nanoparticles, ACE inhibitors; circular dichroism, *in-vitro* release kinetics

1. Introduction

Isoleucine-Proline-Proline (IPP) and Leucine-Lysine-Proline (LKP) are both Angiotensin Converting Enzyme (ACE) inhibitors, which have the potential to either maintain normal blood pressure and prevent escalation of hypertension or be used for the treatment of mild or pre-hypertension (Bütikofer, Meyer, Sieber, Walther, & Wechsler, 2008; Fujita & Yoshikawa, 1999). ACE is responsible for the cleavage of a His-Leu dipeptide from Angiotensin I (Ang I), converting it to Angiotensin II (Ang II), causing vasoconstriction, increase in sympathetic tone, vasopressin release and aldosterone secretion (Maria et al., 2016). ACE inhibitors block this conversion which consequently reducing the Ang II levels and also inhibiting the catabolism of a vasodilatory peptide, bradykinin (Maria et al., 2016). In recent years, bioactive peptides isolated from food have attracted market attention for their physiological effects, but clinical applications are still limited due to variable or poor permeation when administered orally. These limiting factors are due to a number of issues such as insufficient gastric residence time, poor permeation across the intestinal epithelium and/or solubility or chemical degradation within the gastrointestinal tract (GIT) due to low pH, secretory and intracellular peptidases. The presence of other nutrients can also influence absorption of the tri-peptides in the GIT (Jahan-Mihan, Luhovyy, Khoury, & Harvey Anderson, 2011). Hypotensive effects of these tri-peptides have been demonstrated in the Spontaneously Hypertensive Rat model (Fujita & Yoshikawa, 1999; Nakamura, Yamamoto, Sakai, & Takano, 1995). Results from these studies indicated that both tripeptides do have a pharmacodynamic effect when administered intravenously. However, to administer these tripeptides by the oral route, their permeation needs to be enhanced. A number of techniques have been previously investigated to help overcome such barriers, including carrier systems made of lipids (Pandita, Kumar, Poonia, & Lather, 2014) or polysaccharides (Liu, Jiao, Wang, Zhou, & Zhang, 2008) or the addition of inhibitors and enhancers (Gleeson, Heade,

Ryan, & Brayden, 2015; Maher, Mrsny, & Brayden, 2016). Chitosan in particular, a partially deacetylated polymer consisting of a β- (1, 4)-linked-D-glucosamine residue with amine groups, has been applied successfully in many areas of research (Al-Naamani, Dobretsov, & Dutta, 2016; Koppolu et al., 2014; S. M. Ryan et al., 2013; Sarvaiya & Agrawal, 2015). Chitosan is a good example of a polysaccharide carrier which has been widely used in bioactive encapsulation in the form of nanoparticles (NPs), providing muco-adhesiveness, the ability to open epithelial tight junctions and pH-dependant swelling behaviour (Garcia-Fuentes & Alonso, 2012). Chitosan is positively charged under acidic conditions, to an extent which depends on the degree of deacetylation (DD), the percentage of primary amino groups in the polymer backbone and molecular weight. An increase in DD allows the ionisation of the chitosan, which increases the viscosity, resulting in an extended conformation with more charge repulsion and a more flexible chain (Kumirska et al., 2010; Vozza, Khalid, Byrne, Ryan, & Frias, 2016). For encapsulation purposes, chitosan at high DD is usually selected to allow more possibilities for the bioactive to interact (i.e. increasing molecular mobility) (Szymańska & Winnicka, 2015). Nanoparticle based drug delivery systems have been widely used in the area of encapsulation, using different carrier systems (Vozza et al., 2016). Studies have shown the potential of controlling NP size and surface properties and the resultant formulations have provided site-specific action of the drug at the optimal therapeutic rate and dose (Yun, Cho, & Park, 2013a).

Ionotropic gelation is a physical process used to formulate chitosan nanoparticles using a crosslinker (counterion), tripolyphosphate (TPP). Although the ionotropic process is simple, without the use of organic solvents, it is important to ensure that the intrinsic properties of a peptide are maintained before and after any formulation process occurs. Depending on the formulation and the bioactive, particles with different properties can be obtained. Chitosan nanoparticles for the formulation of peptides such as nisin (Bernela, Kaur, Chopra, & Thakur,

2014; Khan & Oh, 2015), insulin (Mukhopadhyay, Mishra, Rana, & Kundu, 2012), Z-DEVD-FMK (Aktaş et al., 2005), calcitonin (S. M. Ryan et al., 2013) and dermaseptin (Medeiros, Joanitti, & Silva, 2014) were formulated and their bioactivity was assessed after the formulation processes have taken place. Sarmento et al. (2007) investigated the possible interactions and changes of secondary structure of insulin when encapsulated into a chitosan nanoparticle using FT-IR and circular dichroism, they found that the intrinsic property of insulin was maintained after encapsulation. The interaction of chitosan with the encapsulated bioactive is an important aspect which can predict the suitability of future formulations and may help provide a more systematic approach to future bioactive encapsulation.

In this study, the preformulation and formulation steps were assessed for IPP and LKP encapsulated into chitosan NPs. The different characteristic properties of IPP, LKP and the loaded nanoparticles were investigated with the aim of establishing a better fundamental understanding of any physicochemical changes of the bioactive before and after the formulation process.

2. Materials and Methods

Both peptides, LKP (Mw 356.47, purity = 97% according to the manufacturer's specifications) and IPP (Mw 325.41, purity = 97% according to the manufacturer's specifications) were synthesised by ChinaPeptides Co. Ltd, (Shanghai, China). CL113 (Mw = 110 kDa, deacetylation degree = 86% according to manufacturer's specifications) was obtained from Pronova Biopolymer (Norway). CellTitre 96® AQ_{ueous} One Solution Cell Proliferation Assay was supplied by Promega (Madison, USA). Caco-2, heterogeneous human epithelial colorectal adenocarcinoma cells were obtained from European Collection of Cell Cultures (Salisbury, UK). HepG2, human liver cancer cells were obtained from American Type Culture Collection. Ultrapure water was used for all experiments and was obtained from a Milli-Q water purification system (Millipore Corporation, USA). TPP

(sodium tripolyphosphate), Angiotensin-I converting enzyme (from rabbit lung), captopril, N-α-hippuryl-L-histidyl-L-leucine hydrate salt (HHL) and all other reagents were purchased from Sigma Aldrich, Ireland.

2.1 Molecular Modelling

Molecular models were built for chitosan, IPP and LKP using Chem3D Pro software (version 12.0.2.1076 developed by ChembridgeSoft corporation). Refinement of the structures by minimisation of conformational energy was performed using MM2 (Molecular Mechanics) force field (Burkert & Allinger, 1982). The exact structure of chitosan was translated from SMILES (chemicalize.org, 2016) to Chem3D Pro software.

2.2 Conformational analysis

Circular dichroism was performed using a Jasco J-810 Spectropolarimeter with a 150 W Xe arc lamp and an operating range from 163 to 900 nm. This measured the absorption difference between left and right circularly polarized light for an electronic transition. A quartz cell with a light-path length of 0.5 cm was used for all measurements. IPP and LKP were measured in water and chitosan in pH3 acetate buffer solution to mimic formulation conditions.

2.3 LKP and IPP-loaded NPs formulation and physicochemical characterisation

A mixture amount design was produced using two variable parameters (CL113 and TPP) composed of 5 experiments (table 1).

Table 1 Mixture amount design of LKP and IPP nanoparticles in which the concentrations of CL113 and TPP were the variable parameters in the model

Formulation	Ratio (CL113:TPP)	Cl113 (mg/mL)	TPP (mg/mL)	Peptide (µg/mL)
A	8:1	1.64	0.21	100
B	6:1	1.58	0.27	100

C	5:1	1.52	0.33	100
D	4:1	1.45	0.40	100
E	3:1	1.39	0.46	100

Preliminary studies showed concentrations within the range of 1.3-1.6 mg/mL chitosan and 0.2-0.5 mg/mL TPP produced unloaded nanoparticles with the best physicochemical characteristics in terms of size 100-500 nm (des Rieux, Fievez, Garinot, Schneider, & Préat, 2006), polydispersity (PDI) <0.4 (Abdel-Hafez, Hathout, & Sammour, 2014a) and zeta potential (ZP) >30 mV (Lakshmi & Kumar, 2010) for an oral drug delivery system. Therefore, these concentration ranges were selected for this study.

Stock solutions of 10 mg/mL CLL113 and TPP were prepared. CL113 was dispersed in acetate buffer (pH 3) and TPP in 0.01 M sodium hydroxide solution. The stock solutions of CL113 and TPP were diluted to different concentration ratios following a third order polynomial mixture amount design (table 1). A fixed concentration of 0.1 mg/mL peptide was added to the diluted TPP solutions. The TPP-peptide solution was added dropwise to the CL113 solution while stirring. NPs were separated using ultrafiltration-centrifugation (Centriplus YM-30, MWCO of 30kDa, Millipore, USA). The volume of the solution in the filtrate vial was measured and the filtrate was assayed for the amount of LKP or IPP by Reverse Phase High Performance Liquid Chromatography (RP-HPLC). The wet pellet was re-suspended in purified water and immediately characterised using a range of physico-chemical techniques. The nanoparticle size and electrophoretic mobility measurements were performed using folded capillary cells in a Nanosizer ZS fitted with a 633 nm laser (Malvern Instruments Ltd.). Each analysis was carried out at 25°C with the equilibration time set to 2 min. The experimental design and data analysis was performed using Minitab 17 software (Minitab Inc, USA). The regression coefficients and responses for IPP and LKP were analysed and compared.

166 2.4 Determination of encapsulation efficiency peptide-loaded nanoparticles

167 The encapsulation efficiency (EE %) of the peptides in the NPs was calculated by the indirect
168 method (Calvo, Remunan-Lopez, Vila-Jato, & Alonso, 1997). The supernatant was assayed
169 for the content of LKP or IPP by RP-HPLC. The RP-HPLC analysis was performed on a
170 Waters 1525 pump (Waters, Milford, Massachusetts) with a Photo Diode Array detector 2487
171 (Waters) using a Luna C18 column (5 µm, 250 mm x 4.6 mm, Phenomenex). Analytes were
172 detected at the wavelength of λ_{max}= 220 nm (LKP) and 215 nm (IPP). For LKP; the column
173 was eluted at a flow rate of 1 mL min^{-1} with an isocratic system (15% Acetonitrile, 0.05%
174 TFA in 84.95% water) and 10 µL injection volume. For IPP; the column was eluted at a flow
175 rate of 0.8 mL min^{-1} with an isocratic system (20% Acetonitrile, 0.05% TFA in 79.95%
176 water) and 5 µL injection volume. The EE % was calculated using the following equation:

177 $$\text{EE } \% = \frac{(\text{Total amount Peptide} - \text{free amount Peptide in supernatant})}{\text{Total amount of Peptide}} x\ 100 \quad (1)$$

178 2.5 Comparison of ACE inhibition for peptides and nanoparticles

179 ACE inhibition was measured for IPP and LKP over the concentration range 0.001-50 µM,
180 using an ACE inhibition assay with HHL as substrate (Henda et al., 2013; Lahogue, Réhel,
181 Taupin, Haras, & Allaume, 2010). Briefly, HHL (5 mM) was dissolved in pH 8.3 buffer (0.1
182 M borate buffer in 0.3 M NaCL). 100 µL substrate solution and 25 µL inhibitor (peptides or
183 peptide loaded NPs) were incubated for 10 min at 37°C. 10 µL ACE solution (100 mU/mL)
184 were then added, incubated for 30 min and terminated using 100 µL of 1 M HCL. HPLC was
185 performed using a C8 column (2.7 µm, 3.0 x 100 mm, Agilent Technologies UK & Ireland
186 Ltd) at a wavelength of 228 nm. An isocratic method was used at a flow rate of 0.4 $mL.min^{-1}$,
187 25% Acetonitrile, 0.1% TFA in 74.9% water for 5 min. Captopril was used as the control.
188 The % of ACE activity was calculated:

189 $$ACE\ inhibition\ \% = 1 - \left(\frac{A^{inhibitor}}{A^{blank}}\right) * 100 \quad (2)$$

where $A^{inhibitor}$ and A^{blank} are the peak areas of HA (product of HHL) and negative control. The IC_{50} of the inhibitor was determined using the Hill Slope equation (Prism 5, GrapPad Software Inc., USA). The ACE inhibition assay was also performed on the released peptide from the loaded NP at the last sample point (720 min SIF). Loaded NPs (19.5 mg in 10 mL water) were subjected to sonication for 2 min at 40% amplitude (Branson Ultrasonics; Ultrasonic processor VCX-750W, Wilmington, North Carolina, USA). Peptides were then isolated using centrifugation and the supernatant was quantified using HPLC, and diluted to 10 μM to investigate any change of inhibition activity compared to the native peptides using HHL substrate.

2.6 Cytotoxicity assessment of LKP and IPP by MTS

Caco-2 (passage 24-26) and HepG2 (passage 32-34) cell lines were seeded at a cell density of 2 x 10^4 cells/well and cultured on 96 well plates in DMEM and EMEM respectively, supplemented with 10% foetal bovine serum, 1% $_L$-glutamine, 1% penicillin-streptomycin and 1% non-essential amino acids, and incubated at 37°C in a humidified incubator with 5% CO_2 and 95% O_2. Caco-2 cells were exposed to IPP, LKP, unloaded NPs and IPP and LKP loaded nanoparticles (in serum free media) for 4 h (Neves, Martins, Segundo, & Reis, 2016) to mimic intestinal exposure and HepG2 cells for 72 h (Brayden, Gleeson, & Walsh, 2014) to mimic liver exposure at concentrations (1, 5 and 10 mM for IPP/LKP and NPs). 0.05 % Triton X-100™ (detergent) was used as a positive control. After exposure, treatments were removed and replaced with MTS (3-(4, 5-dimethylthiazol-2-yl)-5-(3-carbo xymethoxyphenyl)-2-(4-sulfophenyl)-2H-tetrazolium). Optical density (OD) was measured at 490 nm. Each value presented was normalised against untreated control and calculated from three separate experiments, each of which included six replicates. Data was analysed using one-way ANOVA with Dunnett's multiple comparison test.

2.7 *In-vitro* controlled release analysis of peptides

The release of the peptide from chitosan NPs at the optimal ratio of CL113:TPP (ratio 6:1 (LKP), ratio 4:1 (IPP)) was studied by a dialysis method, 2 h in simulated gastric fluid (SGF) followed by 4 h in simulated intestinal fluid (SIF). Freeze dried NPs in 2.5% trehalose, equivalent to 10 mL formulation, were placed in a cellulose dialysis bag (cutoff molecular weight 10 kDa, Spectra-Por® Float-A-Lyzer® G2). The dialysis bag was placed into the receptor compartment containing the dissolution medium (40 mL), which was set at 100 rpm and maintained at 37°C using a thermostatic shaker. This procedure was performed without enzymes in accordance with British Pharmacopoeia, 2016, but with the exception of using a dialysis membrane. SGF was composed of 0.1 M HCL and SIF was the buffering stage composed of 1 volume of 0.2 M trisodium phosphate dodecahydrate and 3 volumes of 0.1 M HCL (adjusted to pH 6.8), without enzymes (British Pharmacopoeia, 2016) . Samples were withdrawn at different time intervals; 1 mL of sample fluid was removed at each time point and replaced with 1 mL simulated buffer. The samples were measured using RP-HPLC (method 5.2.2).

$$\text{cumulative release } \% = \frac{\text{Peptide release}}{\text{Peptide initial}} * 100 \qquad (3)$$

where peptide (LKP/IPP) release and initial represents the concentration of peptide (LKP/IPP) release and the amount of peptide (LKP/IPP) initially loaded into the NPs, respectively.

2.7.1 Release kinetics

The release kinetics of the peptide formulation under the SGF and SIF sequential controlled release experiments were fitted using diffusive models derived from swellable systems (Siepmann & Peppas, 2011).

For the SGF:

$$\frac{M_t}{M_\infty} = ks_1 * \left(\sqrt{time}\right) + ks_2 * time \qquad (4)$$

where M_t is the diffused mass at a given time, M_∞ is the asymptotic diffused mass at infinite time, ks_1 and ks_2 are diffusive and relaxation rate constants.

For the SIF:

$$\frac{M_t}{M_\infty} - \frac{M_{120}}{M_\infty} = ki_1 * \left(\sqrt{time - 120}\right) + ki_2 * (time - 120) \quad (5)$$

where M_{120} is the predicted diffused mass at the time of changing from SGF to SIF (120 min), ki_1 and ki_2 are diffusive and relaxation rate constants.

The model building process involved:

1. A model with k_{i1}, k_{i2}, k_{s1} and k_{s2} for each peptide was built using nonlinear regression and all the available data.
2. A set of candidate reduced models were produced by following two model reduction strategies:
   a. If any of the parameters was not significantly different between peptides, a new model with common parameters for both LKP and IPP was fitted.
   b. If the parameters k_{i2}, or k_{s2} were not statistically significant, a new candidate model was fitted by reducing the Peppas model in equations 4 or 5 to a model without the relaxation related term.
3. The resulting reduced model was compared with the previous model through a log-likelihood ratio test (Welham & Thompson, 1997).
4. Steps 2 and 3 were repeated until a model that explained the experimental data with the same ability as the model described in bullet point (1) with a minimum set of parameters.

The nonlinear regression methods from the R software were used (R Core Team, 2015).

3. Results

3.1 Molecular modelling of peptides

Molecular modelling was used to evaluate the conformational structure of the tripeptides. Molecular modelling calculates the energy of a particular molecular structure and then

iteratively adjusts the energy through changes in bond lengths and angles to determine the minimum energy structure (Mulloy, Forster, Jones, & Davies, 1993). For MM2, the following are taken into account:

- A charge-dipole interaction term
- A charge-dipole interaction term
- A quartic stretching term
- Cutoffs for electrostatic and van der Waals terms with 5th order polynomial switching function
- Automatic pi system calculations when necessary
- Torsional and non-bonded constraints

The resultant energy minimised structures are shown in Figure 1.

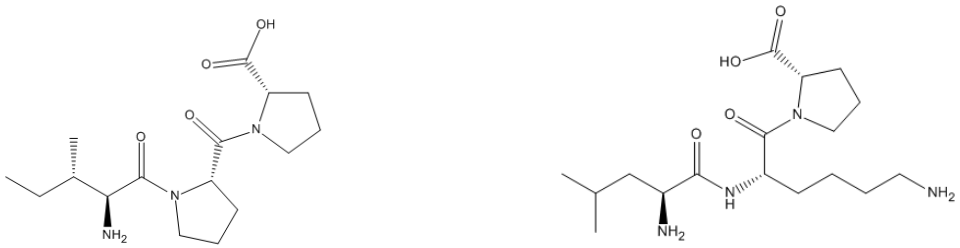

(a) **(b)**

Figure 1 (a) IPP and (b) LKP chemical structure at its minimised energy state

The minimised total energy calculated for IPP, LKP and chitosan were 35.60 kcal/mol, 8.57 kcal/mol and 381.02 kcal/mol, respectively (table 2). LKP was found to have a significantly lower energy compared to IPP and chitosan. Other significant differences were found in the bending, indicating that for chitosan and IPP, more energy is required to deform an angle from its equilibrium state, as presented in table 2. In addition, the torsion for all three components showed significant difference for dihedral angles (torsionals,) which is the energy needed to overcome torsional strain, IPP having more torsional strain than LKP.

Table 2: MM2 analysis of LKP, IPP and chitosan

	LKP (kcal/mol)	IPP (kcal/mol)	CL113 (kcal/mol)
Stretch	1.50	1.95	22.64
Bend	12.04	24.26	157.23
Stretch-Bend	0.39	0.43	13.65
Torsion	5.50	15.78	124.29
Non-1,4 Van der Waals	-11.23	-7.77	-151.22
1,4 Van der Waals	12.35	12.95	219.93
Dipole/Dipole	-11.98	-11.99	-5.50
Total Energy	8.57	35.6	381.02

3.2 Conformational analysis

To further confirm the conformation of the peptides, circular dichroism was used for both peptides and CL113. For our experiment, the spectral range (260–180 nm) was used to measure the light absorption of the peptide bonds to investigate the chiral structure of peptides.

As presented in figure 2, CD showed similar spectral profiles for LKP and chitosan over the range 180-260 nm, but markedly different for IPP, indicating different stable side-chain-specific conformations, an unordered peptide structure for IPP and a (disordered) β-strand-like structure for LKP (Gokce, Woody, Anderluh, & Lakey, 2005; Rath, Davidson, & Deber, 2005).

CL113 is a large polysaccharide which has been reported to adopt a very tight twisted secondary structure, found to be even more complex in aqueous solutions, causing it to unwind the helical structure to a more disordered structure (Y. Wu et al., 2004). Such disorder is evident in figure 2(a). Spectra of LKP and IPP are in accordance with Rath et al. 2005, showing a β-strand conformer for LKP and random coil-like structure for IPP.

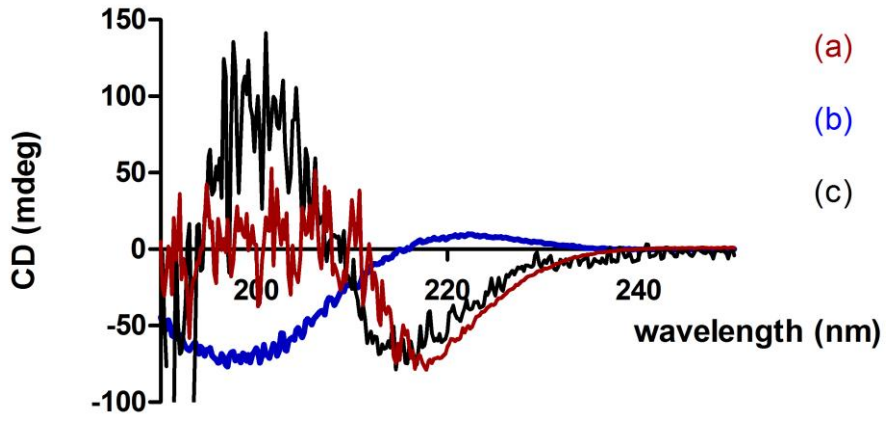

300

301 **Figure 2** CD spectra of (a) chitosan, (b) LKP and (c) IPP

302 3.3 Formulation and physicochemical characteristics of LKP and IPP nanoparticles

303 In the formulation process (section 2.4), the tripeptide was added to the TPP basic solution,
304 higher than its isoelectric point, to allow ionisation (determined using isoelectric.ovh.org
305 (2016): LKP = 9.07, IPP = 5.98, TPP = 6.59) predominately protonating the carboxyl (O^-)
306 and interacting with the deprotonated amine of acidic chitosan, NH_3^+ (Naik 2015), as
307 illustrated in figure 3.

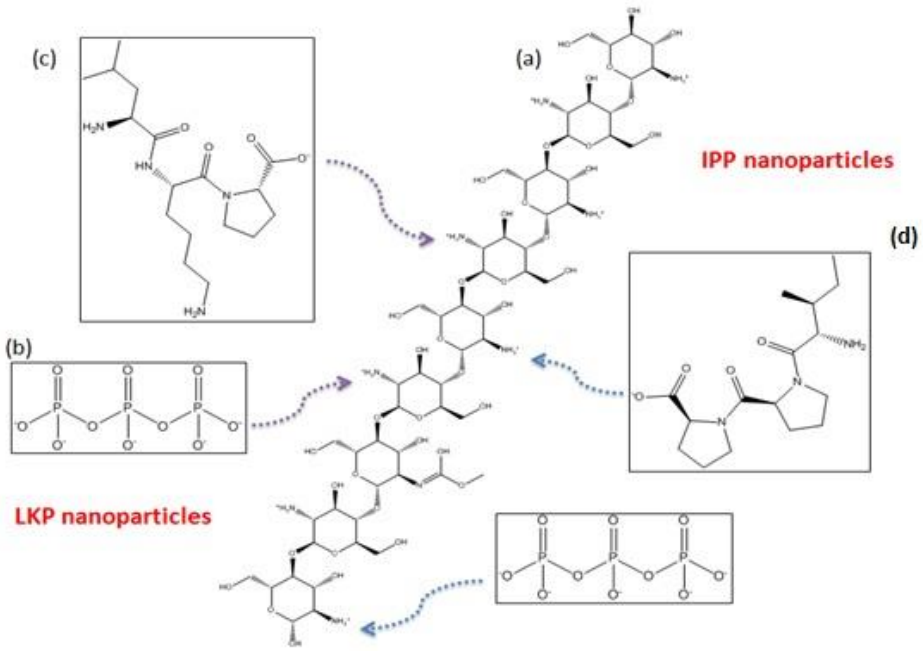

Figure 3 Schematic of LKP and IPP formulation into nanoparticles where (a) chitosan is protonated in acidic conditions and (b) TPP (c) LKP and (IPP) are oxidised in basic conditions.

The ratio between the polymer and crosslinker is the key to a high EE % (Patil, Marapur, Gurav, & Banagar, 2015). The same mixture amount design at different ratios of CL113 and TPP was used for both LKP and IPP in order to help choose the best formulation with optimal characteristics of delivery (table 2). Different bioactives interact differently to different ratios of CL113 and TPP for example depending on the size and charge of the encapsulated bioactive. The PDI, ZP value and EE % were measured for both LKP and IPP nanoparticles at different ratios, further analysed using experimental design analysis (see table 4). Formulation B (ratio 6) gave the best physicochemical characteristics with high EE % (65%). Additionally, formulation D (ratio 4) gave the best physicochemical characteristics with high EE % (44.8%).

Table 3: Physicochemical results of size (nm), ZP (mV), PDI, EE % and LC % of loaded IPP and LKP nanoparticles

Formulation	Peptide at 100µg/ml	Size (nm)	ZP (mV)	PDI	EE %	LC %
A	IPP	209 ±18	36.6 ±2	0.5 ±0.1	22.6 ±7	1.2 ±0.2
	LKP	207 ±73	38.2 ±5	0.4 ±0.2	40.9 ±11	2.2 ±0.1
B	IPP	173 ±15	32.8 ±2	0.3 ±0.1	30.2 ±12	1.6 ±0.4
	LKP	166 ±14	31.6 ±2	0.3 ±0.1	65.1 ±4	3.3 ±0.0
C	IPP	135 ±23	30.1 ±3	0.3 ±0.1	35.3 ±9	1.8 ±0.0
	LKP	145 ±13	31.6 ±4	0.4 ±0.1	45.3 ±14	2.3 ±0.8
D	IPP	143 ±16	29.6 ±2	0.3 ±0.1	44.8 ±6	3.0 ±0.1
	LKP	145 ±9	32.5 ±4	0.4 ±0.1	50.8 ±7	2.7 ± 0.3
E	IPP	113 ±10	28.6 ±6	0.2 ±0.1	43.9 ±4	2.3 ±0.1
	LKP	125 ±10	29.3 ±3	0.5 ±0.3	46.9 ±5	2.8 ± 0.2

The third order polynomial regression coefficients of LKP and IPP parameters, shown in table 4, were analysed and compared from the results in table 3. For size, PDI and zeta potential, a similar trend was observed, showing a positive coefficient for CL113 and TPP and a negative coefficient for the CL113 and TPP interaction (CL113*TPP).

A reduction in size, PDI and ZP was observed with the interaction of CL113*TPP, whereby TPP was found to have the strongest effect with the highest coefficient (table 3). In general, all experiments were found to produce nanoparticles within the optimal physicochemical characteristics for oral delivery systems (El-Shabouri, 2002; Sarvaiya & Agrawal, 2014; Yun, Cho, & Park, 2013b). These physicochemical results are in agreement with other studies, previously reporting an optimal ratio of chitosan: TPP between 4-8: 1 (Abdel-Hafez, Hathout, & Sammour, 2014b; Calvo et al., 1997). For EE %, a different response was found, whereby TPP and CL113 both showed a negative coefficient and CL113*TPP a positive, indicating a reduction of EE % with CL113 and TPP on its own and an increase of EE % with the

interaction of CL113 and TPP. LKP was seen to have a more pronounced positive coefficient for CL113*TPP (1811) compared to IPP (715.7), indicating a stronger interaction for LKP.

Table 4 Coefficients of polynomial regression equation of LKP vs IPP for normalised (a) Size, (b) PDI, (c) zeta potential and (d) EE % for LKP and IPP where Coef is coefficient

	LKP	**IPP**
	Coefficient	**Coefficient**
(a)		
CL113	207.1	212.0
TPP	1366.7	1238.6
CL113*TPP	-1230.1	-1165.1
(b)		
CL113	0.5	0.5
TPP	9.6	3.2
CL113*TPP	-7.0	-2.9
(c)		
CL113	30.9	30.9
TPP	181.5	177.5
CL113*TPP	-150	-149.9
(d)		
CL113	-3.5	-8.7
TPP	-648.5	-167.9
CL113*TPP	544.8	209.1

Taking this into account, the EE % was found to be different for IPP and LKP, within the experimental conditions. Results showed that, for formulation B (Ratio 6:1 CL113: TPP), a high EE % was produced for LKP (65 ±4%) and a lower EE % of 30 ±12% for IPP. A decrease of the CL113: TPP ratio for IPP nanoparticles resulted in an increase of encapsulation, as shown in Figure 3. Formulation D (Ratio 4:1 CL113: TPP) produced the best IPP EE % with lowest variability (44 ±6%).

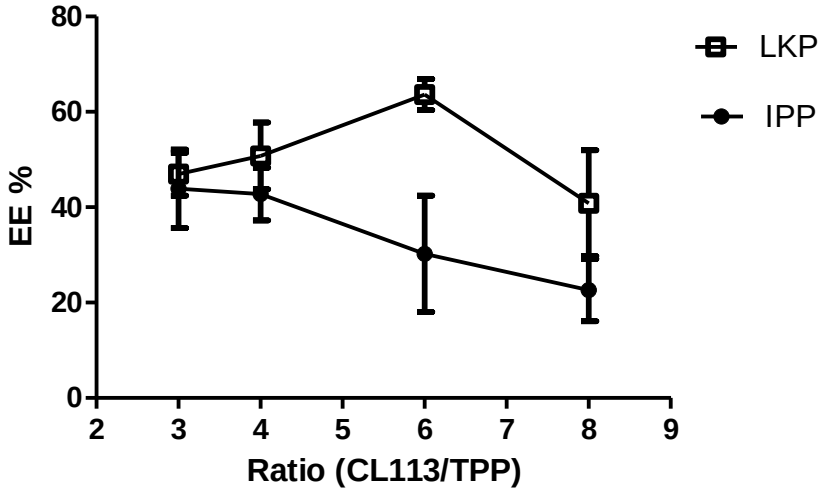

348

349 **Figure 4** Comparison of encapsulation efficiency of LKP-loaded nanoparticles and IPP-
350 loaded nanoparticles at different ratios (CL113/TPP)

351 3.4 Comparison of ACE inhibitory activity of LKP and IPP and nanoparticles

352 The ACE inhibitory activity of LKP and IPP were compared to captopril, a known ACE
353 inhibitor, using the substrate, HHL. A concentration-response curve was plotted to determine
354 the IC_{50} values (figure 5). The IC_{50} for captopril, LKP and IPP were calculated to be 0.006 ±
355 0.002 μM, 0.36 ± 0.01 μM and 3.1 ± 0.6 μM, respectively. The lowest IC_{50} value was
356 obtained for captopril, followed by LKP than IPP.

357

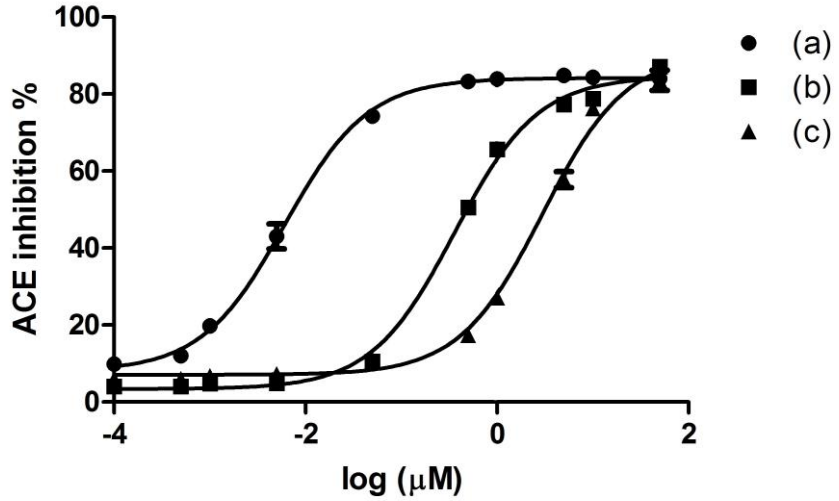

358

359 **Figure 5** ACE inhibitory effect on (a) Captopril (b) LKP and (c) IPP. Data are expressed as
360 the mean ± SD. Differences among groups were evaluated by one-way ANOVA. For all
361 measurements, six replicates for three separate experiments were taken for data analysis.
362 When comparing all three ACE inhibitors, a significant difference is observed at 95%
363 confidence interval (table 5). The ACE inhibitory effects (%) of the peptides released from
364 the nanoparticles were also determined. The amounts of peptide released from the NPs were
365 190 μM LKP and 102 μM IPP. Peptides were diluted to 10μM and were measured for ACE
366 inhibition using the same assay. A 10μM peptide dose of freshly loaded NPs was sonicated
367 for 1 min without pulse break and ACE inhibition measured for IPP (84± 6%) and LKP (85±
368 3%). Peptide from controlled release experiments was also collected and assayed for ACE
369 inhibition, resulting in equivalent LKP (83± 7%) and IPP (82± 5%) bioactivity. Furthermore,
370 these estimates are comparable to the bioactivity of equivalent doses of fresh IPP and LKP
371 reported in figure 5 (~80%). These two results confirm that the peptides retained their
372 bioactivity even after the nanoencapsulation and release process.

373

374 **Table 5** Comparison of the IC_{50} of LKP and IPP at 95% confidence intervals

	Lower (μM)	Est. (μM)	Upper (μM)

Captopril	0.005	0.006	0.007
IPP	2.336	2.819	3.301
LKP	0.309	0.367	0.425

3.4 Comparison of Cytotoxicity of LKP and IPP

In vitro cytoxicity assessment was performed in Caco-2 and HepG2 cell lines at different exposure times, to mimic the gastro intestinal and liver exposure of the nanoparticles. It has already been reported in the two cell lines that, at therapeutic doses of LKP and IPP (1, 5 and 10 mM), no cytotoxicity was observed (Gleeson et al., 2015). Using the same therapeutic dose ranges, IPP and LKP nanoparticles were tested on Caco-2 and HepG2 cell lines and no significant decrease of cell viability was found compared to the negative control using the MTS viability assay (figure 6).

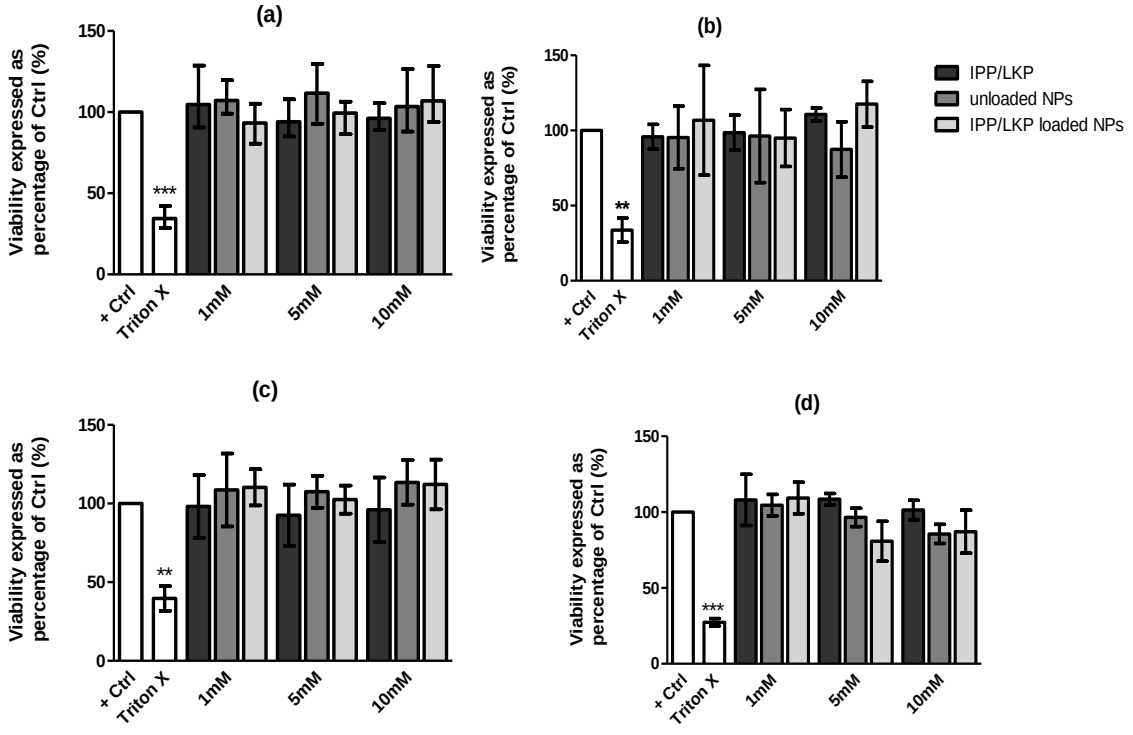

Figure 6 Comparison of cytotoxicity of LKP formulations, as measured using the MTS assay, in (a) Caco2 cell lines 4h exposure and (b) HepG2 cell lines 72h exposure. IPP formulations exposed to (c) Caco2 cell lines exposed to 4h and (d) HepG2 cell lines exposed to 72h. Triton X (0.05%) and 100% cell viability (no treatment) were used as the positive and

negative control. Data were expressed with 1-Way ANOVA with Dunnetts's post-test *** P< 0.001, ** P< 0.01. Each value represents the mean ±SD. n = 3 independent experiments for each concentration and time point with replicates of three.

3.5 *In-vitro* release kinetics of IPP and LKP-loaded nanoparticles

The comparative release behaviour of LKP and IPP nanoparticles was studied in SGF and SIF. *In-vitro* controlled release of IPP and LKP nanoparticles showed an initial burst release in the first 2 h at pH 1.2, followed by a 4 h sustained profile at pH 6.8, such that, after 6 h, a cumulative release up 95% was observed for both peptide systems, showing a similar end result.

To further understand the release mechanism of IPP and LKP nanoparticles, the dissolution experimental results were fitted using the Peppas kinetic model (Section 2.8.1, (4) and (5)). This model is based on a diffusion-controlled phenomenon, and is commonly used to describe the release profile of polymer based delivery systems (Pandita et al., 2014; Wilson et al., 2010; Jie Wu, Ding, Chen, Zhou, & Ding, 2014). For our experiment, the model for relaxation release (for swellable systems) was observed to fit the experimental observations well. Figure 7 presents the obtained results fitted using a nonlinear regression equation, a modified Higuchi /Peppas equation reported by Siepmann & Peppas (2011, shown in section 2.7.1 (equation 4 and 5).

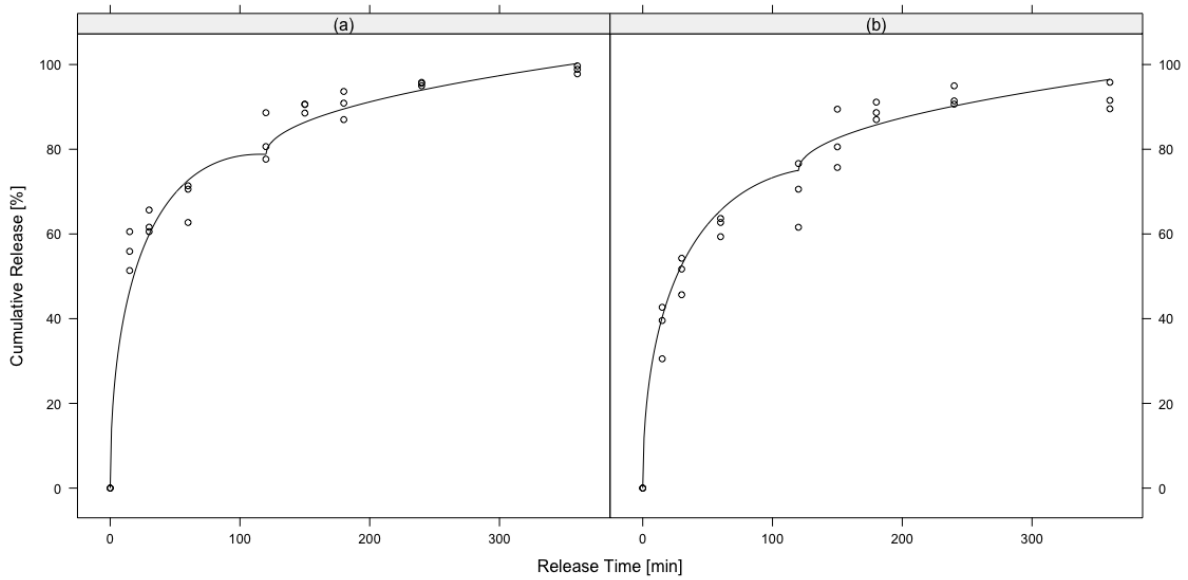

407

408 **Figure 7** Release studies of (a) IPP-loaded and (b) LKP-loaded nanoparticles exposed for a
409 total time of 720 min (6h) :120 min in SGF followed by 240 min in SIF separated by dashed
410 lines (n= 3).

411 Table 6 presents the fitted values for the rate constants, k_{s1}, k_{s2}, according to Equations 4 and
412 5 for LKP and IPP nanoparticles in each simulated GI region. This model predicted the
413 experimental data well with an estimated R^2 adj of 0.98. For each peptide loaded
414 nanoparticle, a combination of diffusive and relaxation phenomena was observed in the SGF.
415 In this medium, k_{s1} and k_{s2} were significantly different for IPP and LKP. IPP was found to
416 exhibit a higher release rate in the SGF than LKP, a difference of ks_1 = 4.27±0.9 and ks_2
417 =0.34±0.09 of IPP vs LKP SGF release.

418 After 2 h incubation in pH 1.2, the nanoparticles were placed in pH 6.8, SIF. No significant
419 changes were found for the rate constant (ki_1) for both IPP and LKP nanoparticles having a
420 k_{i1} of 1.39 ±0.15. No statistically significant ($p<0.05$) k_{i2} relaxation process parameter was
421 found, and the same rate for LKP and IPP was observed with no significant difference,
422 indicating that, in the small intestine (jejunum) at pH 6.8, diffusion is the primary mechanism

of release for both peptides. ACE inhibition assay was also carried for the last sample (time = 720 min), no change in bioactivity was observed after NP release.

Table 6 Parameter estimates of Equation 4/5 for LKP and IPP. All parameters were statistically significant ($p<0.05$).

Release parameters	Estimate
k_{s1} IPP	$15.65 \pm 0.66\ min^{-1/2}$
k_{s1} LKP	$11.38 \pm 0.66\ min^{-1/2}$
k_{s2} IPP	$-0.76 \pm 0.07\ min^{-1}$
k_{s2} LKP	$-0.42 \pm 0.07 min^{-1}$
k_{i1}	$1.39 \pm 0.16\ min^{-1/2}$
$R^2 adj$	0.98
Residual SE	4.74

4. Discussion

Considering the structural characteristics of IPP and LKP (figure 1), both consist of 3 (LKP) and 4 (IPP) chiral centres. The formulation of chitosan nanoparticles is obtained by an electrostatic interaction of the protonated carboxyl (TPP and peptide) interacting with the deprotonated amine of acidic chitosan (see arrows in figure 4). In addition to this, other non-covalent inter and intra molecular interaction may also take place between chitosan, TPP and peptide. This depends on the number of different hydrogen bond donors (HBD) and acceptors (HBA) available to interact. IPP has 2 HBD and 7 HBA and, LKP has 4 HBD and 8 HBA, presented in table 7. LKP was found to have a factor of 2 more HBD than IPP, which may possibly provide better interaction with CL113, as it contains numerous HBA in its polymeric structure, available to interact with, having a solvent accessible surface area of 2014.39Å. IPP and LKP have solvent accessible surface areas of 518.48 and 587.97Å (chemicalize.org,

2016), respectively, contributing to the differences in encapsulation efficiency, as there is more surface area available for LKP.

Table 7 Number of HBD and HBA for LKP and IPP.

	LKP		IPP	
Bond	**HBD**	**HBA**	**HBD**	**HBA**
R-OH	1	1	1	1
R=O	0	3	0	3
R-N	0	1	0	2
R-NH	1	1	0	0
R-NH2	2	2	1	1

Proteins and polypeptides show strong characteristic CD spectra (Greenfield, 2006) but those of tripeptides have also been reported to be characteristic of stable side-chain specific conformations of such peptides (Gokce et al., 2005). Investigations of tri-alanine, tri-valine, tri-lysine and glycerol conformation indicated more ordered, flat β sheet-like conformations rather than what is typically known for short peptides, random coil (Eker et al. 2003). Proline is a cyclic structure which provides rigidity as it locks its ϕ-backbone dihedral angle at $\sim -75°$, giving proline an exceptional conformational rigidity compared to other amino acid groups (Cheng, Cetinkaya, & Gräter, 2010). It has previously been reported that Proline-rich residues are common recognition sites for protein–protein interaction modules (Zarrinpar, Bhattacharyya, & Lim, 2003). Others reported proline based amino acids to have relatively high intrinsic probability of predominantely existing as the cis rather than the trans conformer of the preceding peptide bond, compared with other amino acids (Young Ah Shin, Seong Jun Han, 1993). As seen in figure 2, LKP and IPP showed different conformational characteristics. The proline-rich residues in IPP cause more rigidity and steric hindrance to the overall structure, ultimately affecting the intra and intermolecular interactions with chitosan. On the other hand, LKP only has one proline residue, which promotes bending of

458 the structure with less overall rigidity, resulting in significantly lower minimised total energy
459 compared to IPP. CD analysis further confirmed such differences, resulting in an inverse
460 spectrum for both peptides; a (disordered) β-strand was found for LKP and an unordered
461 peptide structure was for IPP. Chitosan is a semi crystalline polymer that exhibits
462 polymorphism, in its liquid phase (Kumirska et al., 2010). CD showed a mixed conformation
463 between a μ-helical and β-sheet.
464 LKP loaded nanoparticles were found to produce better overall characteristics for a
465 nanoparticle delivery system, in comparison to the IPP counterpart. LKP nanoparticles
466 showed higher overall encapsulation efficiency and a slower release profile. LKP showed
467 best EE % at a CL113: TPP ratio of 6:1 (Formulation B) and IPP at 4:1 (Formulation D). This
468 can possibly be due to the number of exposed interactive sites the peptide had with chitosan
469 and the conformation the peptide, IPP needing more TPP (i.e. lower ratio CL113: TPP) to
470 increase the overall negative charge for electrostatic interaction amongst chitosan and IPP,
471 presented in table 4. This result for IPP is in agreement with Gan & Wang (2007), who found
472 that an increase of encapsulation was achieved with a decrease of ratio in bovine serum
473 albumin protein. The authors proposed a possible explanation, that the larger TPP mass may
474 increase the solution pH value, ultimately increasing the overall negative surface charge
475 carried by the protein molecules, which enhanced electrostatic interactions (Gan & Wang,
476 2007). Taking this into account, LKP showed the highest EE % at ratio 6:1 (less TPP) and
477 IPP at ratio 4:1 (more TPP).
478 The results of the bioactivity assessment of the peptides are in agreement with the findings of
479 other groups; for example, Henda et al. (2013) reported an IC_{50} value of 0.0151 ± 0.005 μM
480 for captopril and Stanton (2011) reported the IC_{50} value of LKP as 0.32 μM. Different IC_{50}
481 values have been reported for IPP, varying from 1.89 to 5 μM (Siltari, Viitanen,
482 Kukkurainen, Vapaatalo, & Valjakka, 2014; van Platerink, Janssen, & Haverkamp, 2007). It

has been reported that peptides with specific amino acids at the N- and C-terminus have shown variable inhibition activity with ACE (Iwaniak, Minkiewicz, & Darewicz, 2014). Wu et al. (2006) reported the most favourable tripeptides for ACE inhibition; at the C terminus onwards were aromatic acids, to the second position were positively charged amino acids (middle amino acid) followed by hydrophobic amino acids for the N terminus. Taking this into account, LKP follows a middle positively charge amino acid (Lys) with a hydrophobic N terminus (Pro) and IPP only follows a hydrophobic N-terminus (Pro). Both LKP and IPP have shown ACE inhibition, but with different IC_{50} values, whereby LKP exhibits almost 10 fold higher activity *in-vitro* compared to IPP. To confirm that all bioactivity of the peptide was retained after *in-vitro* release studies (spontaneously released NPs); an ACE inhibition assessment of the last sample point was assessed. Results showed no reduction in ACE inhibition compared to the positive control. No degradation or denaturation was observed after in-vitro and control (sonicated release). It has been recently reported that IPP and LKP are stable against low pH, intestinal and liver peptidase, indicating their ability to retain after enzymatic processes (Gleeson et al. 2015). Additionally, MTS cytotoxicity assessment for native and NPs of LKP and IPP found no reduction in cell viability at 1-10 nM concentration.

The *in-vitro* release profiles observed in SGF (2 h) at pH 1.2 and SIF (4 h) at pH 6.8 for 6 h, in both optimal peptide formulations were different. The type of bioactive used and ratio of CL113: TPP are the two driving factors that will contribute to the overall release of the particles. Several groups have reported different release profile of different drugs at different ratios, many demonstrating that, at lower ratio (CL113:TPP), a faster release is observed (Gan & Wang, 2007), although others have found that, at lower ratios (CL113:TPP), a slower release is attained (Kouchak & Azarpanah, 2015; Remuñán-López & Bodmeier, 1997). In this case, for both formulations, a burst followed by relaxation (ks_2) in SGF and a sustained release in the SIF was observed, but with significant differences in rate constants in the SGF

508 (ks_1 and ks_2). IPP showed a significantly faster release in the acidic pH compared to LKP;
509 this can possibly be due to the rigidity and steric hindrance of IPP restricting the interaction
510 with chitosan. The higher burst of release for IPP may possibly signify more loosely bound
511 IPP in/around the nanoparticle. Both IPP and LKP produced the same intestinal rate constant
512 $ki = 1.39\ min^{-1/2}$, consistent with a diffusive release profile. The target site for IPP and LKP
513 absorption is the jejunum in the small intestine. In order for the peptide to provide its
514 inhibitory affect, it needs to bypass the stomach/acid pH and other enzymatic process. For
515 both peptide formulations, over 60% release was observed within the first 2h in the acidic
516 simulated fluid. Similar findings have been reported by Sarmento et al. (2007), and Ryan et
517 al. (2013) demonstrated up to 50 and 40% release from chitosan based formulations. This
518 suggests that an enteric coating will facilitate to prevent release in the stomach.

519 **5. Conclusion**

520 LKP and IPP were successfully encapsulated into chitosan nanoparticles. The molecular
521 modelling, supported by the CD analysis, indicates that LKP is different to IPP, the former
522 showing better interaction with chitosan. Such differences in the structural characteristics of
523 LKP and IPP resulted in differences in the overall encapsulation efficiency and release
524 properties of the bioactive.. LKP and IPP are quite similar as ACE inhibitors, but yet
525 different, demonstrating that the characteristics of drug interaction with chitosan is important
526 and needs to be investigated for any future peptide formulations. Overall LKP was found to
527 have better compatibility with chitosan because of increased flexibility, more hydrogen bond
528 donors, better encapsulation of the peptide with the particle and release compared to IPP
529 nanoparticles. However the release of the bioactive (IPP and LKP) still needs to be further
530 optimised to overcome the burst release in the stomach pH 1.2

531 **Acknowledgement**

This project is funded by an Irish Department of Agriculture Food Institutional Research Measure (FIRM) grant 'NUTRADEL' grant number 11F042. Special thanks to Dr Luke O'Neill for the assistance in structural analysis using circular dichroism.

References

Abdel-Hafez, S. M., Hathout, R. M., & Sammour, O. a. (2014a). Towards better modeling of chitosan nanoparticles production: Screening different factors and comparing two experimental designs. *International Journal of Biological Macromolecules*, *64*, 334–340. http://doi.org/10.1016/j.ijbiomac.2013.11.041

Abdel-Hafez, S. M., Hathout, R. M., & Sammour, O. a. (2014b). Towards better modeling of chitosan nanoparticles production: Screening different factors and comparing two experimental designs. *International Journal of Biological Macromolecules*, *64*, 334–340. http://doi.org/10.1016/j.ijbiomac.2013.11.041

Aktaş, Y., Andrieux, K., Alonso, M. J., Calvo, P., Gürsoy, R. N., Couvreur, P., & Çapan, Y. (2005). Preparation and in vitro evaluation of chitosan nanoparticles containing a caspase inhibitor. In *International Journal of Pharmaceutics* (Vol. 298, pp. 378–383). http://doi.org/10.1016/j.ijpharm.2005.03.027

Al-Naamani, L., Dobretsov, S., & Dutta, J. (2016). Chitosan-zinc oxide nanoparticle composite coating for active food packaging applications. *Innovative Food Science & Emerging Technologies*, *38*, 231–237. http://doi.org/10.1016/j.ifset.2016.10.010

Bernela, M., Kaur, P., Chopra, M., & Thakur, R. (2014). Synthesis, characterization of nisin loaded alginate-chitosan-pluronic composite nanoparticles and evaluation against microbes. *LWT - Food Science and Technology*, *59*(2P1), 1093–1099. http://doi.org/10.1016/j.lwt.2014.05.061

Brayden, D. J., Gleeson, J., & Walsh, E. G. (2014). A head-to-head multi-parametric high content analysis of a series of medium chain fatty acid intestinal permeation enhancers

557 in Caco-2 cells. *European Journal of Pharmaceutics and Biopharmaceutics*, *88*(3), 830–
558 839. http://doi.org/10.1016/j.ejpb.2014.10.008
559 British Pharmacopoeia. (2016). Dissolution for delayed release of solid dosage forms
560 (method B). *British Pharmacopoeia*. london: TSO.
561 Burkert, U., & Allinger, N. L. (1982). Molecular Mechanics. *Accurate Molecular Structures*
562 *Their Determination and Importance*, *117*, 1–10. http://doi.org/10.1007/978-90-481-
563 3862-3
564 Bütikofer, U., Meyer, J., Sieber, R., Walther, B., & Wechsler, D. (2008). Occurrence of the
565 angiotensin-converting enzyme inhibiting tripeptides Val-Pro-Pro and Ile-Pro-Pro in
566 different cheese varieties of Swiss origin. *Journal of Dairy Science*, *91*(1), 29–38.
567 http://doi.org/10.3168/jds.2007-0413
568 Calvo, P., Remunan-Lopez, C., Vila-Jato, J. L., & Alonso, M. J. (1997). Novel hydrophilic
569 chitosan-polyethylene oxide nanoparticles as protein carriers. *Journal of Applied*
570 *Polymer Science*, *63*(1), 125–132. JOUR.
571 chemicalize.org. (2016). chemicalize. Retrieved June 24, 2016, from
572 http://www.chemicalize.org/
573 Cheng, S., Cetinkaya, M., & Gräter, F. (2010). How sequence determines elasticity of
574 disordered proteins. *Biophysical Journal*, *99*(12), 3863–3869.
575 http://doi.org/10.1016/j.bpj.2010.10.011
576 des Rieux, A., Fievez, V., Garinot, M., Schneider, Y. J., & Préat, V. (2006). Nanoparticles as
577 potential oral delivery systems of proteins and vaccines: A mechanistic approach.
578 *Journal of Controlled Release*. 116 (1), 1-27.
579 http://doi.org/10.1016/j.jconrel.2006.08.013
580 Eker, F., Griebenow, K., & Schweitzer-Stenner, R. (2003). Stable conformations of
581 tripeptides in aqueous solution studied by UV circular dichroism spectroscopy. *Journal*

582 *of the American Chemical Society*. 125(27), 8178-85. http://doi.org/10.1021/ja034625j
583 El-Shabouri, M. . (2002). Positively charged nanoparticles for improving the oral
584 bioavailability of cyclosporin-A. *International Journal of Pharmaceutics*, *249*(1–2),
585 101–108. http://doi.org/10.1016/S0378-5173(02)00461-1
586 Fujita, H., & Yoshikawa, M. (1999). LKPNM: A prodrug-type ACE-inhibitory peptide
587 derived from fish protein. *Immunopharmacology*, *44*(1–2), 123–127.
588 http://doi.org/10.1016/S0162-3109(99)00118-6
589 Gan, Q., & Wang, T. (2007). Chitosan nanoparticle as protein delivery carrier-Systematic
590 examination of fabrication conditions for efficient loading and release. *Colloids and*
591 *Surfaces B: Biointerfaces*, *59*(1), 24–34. http://doi.org/10.1016/j.colsurfb.2007.04.009
592 Garcia-Fuentes, M., & Alonso, M. J. (2012). Chitosan-based drug nanocarriers: Where do we
593 stand? *Journal of Controlled Release*, *161*(2), 496–504.
594 http://doi.org/10.1016/j.jconrel.2012.03.017
595 Gleeson, J. P., Heade, J., Ryan, S. M. M., & Brayden, D. J. (2015). Stability, toxicity and
596 intestinal permeation enhancement of two food-derived antihypertensive tripeptides, Ile-
597 Pro-Pro and Leu-Lys-Pro. TL - 71. *Peptides*, *71 VN-r*, 1–7. JOUR.
598 http://doi.org/10.1016/j.peptides.2015.05.009
599 Gokce, I., Woody, R. W., Anderluh, G., & Lakey, J. H. (2005). Single peptide bonds exhibit
600 poly(Pro)II (“random coil”) circular dichroism spectra. *Journal of the American*
601 *Chemical Society*, *127*(27), 9700–9701. http://doi.org/10.1021/ja052632x
602 Greenfield, N. J. (2006). Using circular dichroism spectra to estimate protein secondary
603 structure. *Nature Protocols*, *1*(6), 2876–90. http://doi.org/10.1038/nprot.2006.202
604 Henda, Y. Ben, Labidi, A., Arnaudin, I., Bridiau, N., Delatouche, R., Maugard, T., …
605 Bordenave-Juchereau, S. (2013). Measuring angiotensin-I converting enzyme inhibitory
606 activity by micro plate assays: Comparison using marine cryptides and tentative

607 threshold determinations with captopril and losartan. *Journal of Agricultural and Food*
608 *Chemistry*, *61*, 10685–10690. http://doi.org/10.1021/jf403004e
609 isoelectric.ovh.org. (2016). http://isoelectric.ovh.org/. Retrieved June 24, 2016, from
610 http://isoelectric.ovh.org/
611 Iwaniak, A., Minkiewicz, P., & Darewicz, M. (2014). Food-Originating ACE Inhibitors ,
612 Including Antihypertensive Peptides , as Preventive Food Components in Blood
613 Pressure Reduction. *Comprehensive Reviews in Food Science and Food Safety*,
614 *13*(2013), 114–134. http://doi.org/10.1111/1541-4337.12051
615 Jahan-Mihan, A., Luhovyy, B. L., Khoury, D. El, & Harvey Anderson, G. (2011). Dietary
616 proteins as determinants of metabolic and physiologic functions of the gastrointestinal
617 tract. *Nutrients*, *3*(5), 574–603. http://doi.org/10.3390/nu3050574
618 Khan, I., & Oh, D. H. (2015). Integration of nisin into nanoparticles for application in foods.
619 *Innovative Food Science and Emerging Technologies*. 34, 376-384
620 http://doi.org/10.1016/j.ifset.2015.12.013
621 Koppolu, B. P., Smith, S. G., Ravindranathan, S., Jayanthi, S., Suresh Kumar, T. K., &
622 Zaharoff, D. a. (2014). Controlling chitosan-based encapsulation for protein and vaccine
623 delivery. *Biomaterials*, *35*(14), 4382–4389.
624 http://doi.org/10.1016/j.biomaterials.2014.01.078
625 Kouchak, M., & Azarpanah, A. (2015). Preparation and inVitro Evaluation of Chitosan
626 Nanoparticles Containing Diclofenac Using the Ion-Gelation Method. *Jundishapur*
627 *Journal of Natural Pharmaceutical Products.*, *10*(2).
628 Kumirska, J., Czerwicka, M., Kaczyński, Z., Bychowska, A., Brzozowski, K., Thöming, J., &
629 Stepnowski, P. (2010). Application of spectroscopic methods for structural analysis of
630 chitin and chitosan. *Marine Drugs*, *8*(5), 1567–1636. http://doi.org/10.3390/md8051567
631 Lahogue, V., Réhel, K., Taupin, L., Haras, D., & Allaume, P. (2010). A HPLC-UV method

for the determination of angiotensin I-converting enzyme (ACE) inhibitory activity. *Food Chemistry*, *118*(3), 870–875. http://doi.org/10.1016/j.foodchem.2009.05.080

Lakshmi, P., & Kumar, G. A. (2010). Nanosuspension technology: A review. *International Journal of Pharmacy and Pharmaceutical Sciences*. 2(4), 35-40

Liu, Z., Jiao, Y., Wang, Y., Zhou, C., & Zhang, Z. (2008). Polysaccharides-based nanoparticles as drug delivery systems. *Advanced Drug Delivery Reviews*, *60*(15), 1650–62. http://doi.org/10.1016/j.addr.2008.09.001

Maher, S., Mrsny, R. J., & Brayden, D. J. (2016). Intestinal permeation enhancers for oral peptide delivery ☆. *Advanced Drug Delivery Reviews*. http://doi.org/10.1016/j.addr.2016.06.005

Maria, A., Antunes, D. S., Di, R., Guerrante, S., De, J., Ávila, P. C., … Fierro, I. M. (2016). Expert Opinion on Therapeutic Patents Case study of patents related to captopril , Squibb ' s first blockbuster. *Expert Opinion on Therapeutic Patents*, *0*(0), 1–9. http://doi.org/10.1080/13543776.2016.1227321

Medeiros, K. a, Joanitti, G. a, & Silva, L. P. (2014). Chitosan nanoparticles for dermaseptin peptide delivery toward tumor cells in vitro. *Anti-Cancer Drugs*, *25*(3), 323–31. http://doi.org/10.1097/CAD.0000000000000052

Mukhopadhyay, P., Mishra, R., Rana, D., & Kundu, P. P. (2012). Strategies for effective oral insulin delivery with modified chitosan nanoparticles: A review. *Progress in Polymer Science*. http://doi.org/10.1016/j.progpolymsci.2012.04.004

Mulloy, B., Forster, M. J., Jones, C., & Davies, D. B. (1993). N.m.r. and molecular-modelling studies of the solution conformation of heparin. *Biochemical Journal*, *293*(Pt 3), 849–858. http://doi.org/8352752

Nakamura, Y., Yamamoto, N., Sakai, K., & Takano, T. (1995). Antihypertensive effect of sour milk and peptides isolated from it that are inhibitors to angiotensin I-converting

enzyme. *Journal of Dairy Science*, *78*(6), 1253–1257. http://doi.org/10.3168/jds.S0022-0302(95)76745-5

Neves, A. R., Martins, S., Segundo, M. A., & Reis, S. (2016). Nanoscale delivery of resveratrol towards enhancement of supplements and nutraceuticals. *Nutrients*, *8*(3), 1–14. http://doi.org/10.3390/nu8030131

Pandita, D., Kumar, S., Poonia, N., & Lather, V. (2014). Solid lipid nanoparticles enhance oral bioavailability of resveratrol, a natural polyphenol. *Food Research International*, *62*, 1165–1174. http://doi.org/10.1016/j.foodres.2014.05.059

Patil, J., Marapur, S., Gurav, P., & Banagar, A. (2015). *Handbook of Encapsulation and Controlled Release: Chapter 14. Ionotropic Gelation and Polyelectrolyte Complexation Technique: Novel Approach to Drug Encapsulation*. (M. Mishra, Ed.). CRC Press.

R Core Team. (2015). R: A language and environment for statistical computing. R Foundation for Statistical Computing. Austria,Vienna: R Foundation for Statistical Computing,. Retrieved from http://www.r-project.org/

Rath, A., Davidson, A. R., & Deber, C. M. (2005). The structure of "unstructured" regions in peptides and proteins: Role of the polyproline II helix in protein folding and recognition. *Biopolymers - Peptide Science Section*. http://doi.org/10.1002/bip.20227

Remuñán-López, C., & Bodmeier, R. (1997). Mechanical, water uptake and permeability properties of crosslinked chitosan glutamate and alginate films. *Journal of Controlled Release*, *44*(2–3), 215–225. http://doi.org/10.1016/S0168-3659(96)01525-8

Ryan, J. T., Ross, R. P., Bolton, D., Fitzgerald, G. F., & Catherine, S. (2011). Bioactive Peptides from Muscle Sources : Meat and Fish. *Nutrients*, *3*(9), 765–791. http://doi.org/10.3390/nu3090765

Ryan, S. M., McMorrow, J., Umerska, A., Patel, H. B., Kornerup, K. N., Tajber, L., … Brayden, D. J. (2013). An intra-articular salmon calcitonin-based nanocomplex reduces

682 experimental inflammatory arthritis. *Journal of Controlled Release*, *167*(2), 120–129.
683 http://doi.org/10.1016/j.jconrel.2013.01.027
684 Sarvaiya, J., & Agrawal, Y. K. (2014). Chitosan as a suitable nanocarrier material for anti-
685 Alzheimer drug delivery. *International Journal of Biological Macromolecules*, *72C*,
686 454–465. http://doi.org/10.1016/j.ijbiomac.2014.08.052
687 Sarvaiya, J., & Agrawal, Y. K. (2015). Chitosan as a suitable nanocarrier material for anti-
688 Alzheimer drug delivery. *International Journal of Biological Macromolecules*, *72*, 454–
689 465. http://doi.org/10.1016/j.ijbiomac.2014.08.052
690 Siepmann, J., & Peppas, N. A. (2011). Higuchi equation: Derivation, applications, use and
691 misuse. *International Journal of Pharmaceutics*. 418(1), 6-12.
692 http://doi.org/10.1016/j.ijpharm.2011.03.051
693 Siltari, A., Viitanen, R., Kukkurainen, S., Vapaatalo, H., & Valjakka, J. (2014). Does the
694 cis/trans configuration of peptide bonds in bioactive tripeptides play a role in ACE-1
695 enzyme inhibition? *Biologics: Targets and Therapy*, *8*, 59–65.
696 http://doi.org/10.2147/BTT.S54056
697 Szymańska, E., & Winnicka, K. (2015). Stability of chitosan-a challenge for pharmaceutical
698 and biomedical applications. *Marine Drugs*, *13*(4), 1819–46.
699 http://doi.org/10.3390/md13041819
700 van Platerink, C. J., Janssen, H.-G. M., & Haverkamp, J. (2007). Development of an at-line
701 method for the identification of angiotensin-I inhibiting peptides in protein hydrolysates.
702 *Journal of Chromatography. B, Analytical Technologies in the Biomedical and Life*
703 *Sciences*, *846*(1–2), 147–54. http://doi.org/10.1016/j.jchromb.2006.08.052
704 Vozza, G., Khalid, M., Byrne, H. J., Ryan, S., & Frias, J. (2016). *Nutrition - Nutrient*
705 *delivery. In: Nanotechnology in the Food Industry, Volume 5*. (U. K. E. Oxford, Ed.)
706 (1st ed.).

Welham, S. J., & Thompson, R. (1997). Likelihood Ratio Tests for Fixed Model Terms Using Residual Maximum Likelihood. *J. R. Stat. Soc. Ser. B Stat. Methodol.*, *59*(3), 701–714. http://doi.org/10.2307/2346019

Wilson, B., Samanta, M. K., Santhi, K., Kumar, K. P. S., Ramasamy, M., & Suresh, B. (2010). Chitosan nanoparticles as a new delivery system for the anti-Alzheimer drug tacrine. *Nanomedicine: Nanotechnology, Biology, and Medicine*, *6*(1). http://doi.org/10.1016/j.nano.2009.04.001

Wu, J., Aluko, R. E., & Nakai, S. (2006). Structural requirements of angiotensin I-converting enzyme inhibitory peptides: Quantitative structure-activity relationship study of Di- and tripeptides. *Journal of Agricultural and Food Chemistry*, *54*(3), 732–738. http://doi.org/10.1016/j.jmaa.2005.05.084

Wu, J., Ding, S., Chen, J., Zhou, S., & Ding, H. (2014). Preparation and drug release properties of chitosan/organomodified palygorskite microspheres. *International Journal of Biological Macromolecules*, *68*, 107–12. http://doi.org/10.1016/j.ijbiomac.2014.04.030

Wu, Y., Seo, T., Maeda, S., Dong, Y., Sasaki, T., Irie, S., & Sakurai, K. (2004). Spectroscopic studies of the conformational properties of naphthoyl chitosan in dilute solutions. *Journal of Polymer Science, Part B: Polymer Physics*, *42*(14), 2747–2758. http://doi.org/10.1002/polb.20149

Young Ah Shin, Seong Jun Han, and Y. K. K. (1993). Conformational Study on Proline-Containing Tripeptides of Ribonuclease TI. *The Journal of Physical Chemistry*, *97*, 9248–9258.

Yun, Y., Cho, Y. W., & Park, K. (2013a). Nanoparticles for oral delivery: Targeted nanoparticles with peptidic ligands for oral protein delivery. *Advanced Drug Delivery Reviews*, *65*(6), 822–832. http://doi.org/10.1016/j.addr.2012.10.007

Yun, Y., Cho, Y. W., & Park, K. (2013b). Nanoparticles for oral delivery: Targeted nanoparticles with peptidic ligands for oral protein delivery. *Advanced Drug Delivery Reviews*. http://doi.org/10.1016/j.addr.2012.10.007

Zarrinpar, A., Bhattacharyya, R. P., & Lim, W. A. (2003). The structure and function of proline recognition domains. *Science's STKE : Signal Transduction Knowledge Environment*, *2003*(179), RE8. http://doi.org/10.1126/stke.2003.179.re8